

Mechanism for Carbon–Oxygen Bond-Forming Reductive Elimination from Palladium(IV) Complexes

Yao Fu,^{†,‡} Zhe Li,[‡] Shuang Liang,[‡] Qing-Xiang Guo,[‡] and Lei Liu^{*,†}

Key Laboratory of Bioorganic Phosphorus Chemistry & Chemical Biology (Ministry of Education), Department of Chemistry, Tsinghua University, Beijing 100084, People's Republic of China, and Department of Chemistry, University of Science and Technology of China, Hefei 230026, People's Republic of China

Received January 25, 2008

Carbon–oxygen bond-forming reductive elimination from transient Pd(IV) aryl/acetate complexes was recently implicated as the product release step in Pd(II)-catalyzed arene oxygenation reactions. The mechanistic details of C–O bond formation from these Pd(IV) intermediates remain elusive and, therefore, are subjected to a systematic theoretical investigation in the present study. Three proposed mechanisms are examined including (A) pre-equilibrium dissociation of a benzoate ligand followed by reductive elimination from the resulting five-coordinate Pd(IV); (B) direct reductive elimination from the six-coordinate Pd(IV); and (C) dissociation of a pyridyl arm of one cyclometalated ligand followed by internal coupling. Through density functional theory calculations it is suggested that mechanism B is favored over the other two mechanisms. This conclusion is supported by the success of the theoretical model based on mechanism B to reproduce the experimental activation free energy barriers. The same theoretical model also can reproduce the small effect of the solvent polarity and the negative Hammett reaction constant associated with the reductive elimination rates. All of these results suggest that mechanism A should not be involved in the reductive elimination. Furthermore, our calculations explain why the rate of reductive elimination from the Pd(IV) complex of bisphenylpyridine is significantly faster than that from the Pd(IV) complex of bisbenzo[*h*]quinoline.

1. Introduction

Carbon–carbon and carbon–heteroatom bond-forming reductive elimination is a fundamental organometallic transformation involved in a wide variety of transition-metal-catalyzed reactions.¹ Previous elegant studies have intensively probed the mechanisms of bond-forming reductive eliminations at Ni(II),² Pd(II),³ Pt(II),⁴ and Pt(IV)⁵ centers, uncovering distinctly different reaction mechanisms in each system. In contrast, considerably less has been known about the mechanistic picture

of C–C or C–heteroatom reductive elimination from the Pd(IV) complexes.⁶ Attempts to study this process have been impeded by the difficulty of synthesizing stable Pd(IV) complexes as well as by the propensity of Pd(IV) to undergo undesired side reactions. Nonetheless, further investigation into the chemistry of Pd(IV) reductive elimination is of current importance because C–C and C–heteroatom elimination from transient Pd(IV) intermediates has been implicated as the product release step in the recently popularized Pd(II)-catalyzed arene C–H activation/coupling reactions.^{7,8} In this context Sanford and co-workers recently reported fascinating synthesis of a series of Pd(IV) aryl/carboxylate complexes that were remarkably stable at ambient temperatures but underwent clean C–O bond-forming reductive elimination upon thermolysis.⁹ The significance of Sanford's pioneering study is that these novel Pd(IV) complexes enabled

* Corresponding author. E-mail: lliu@mails.tsinghua.edu.cn. Tel: +011-86-10-62780027. Fax: +011-86-62771149.

[†] Tsinghua University.

[‡] University of Science and Technology of China.

(1) Frenking, G., Ed. *Theoretical Aspects of Transition Metal Catalysis*; Springer-Verlag: Berlin, 2005.

(2) (a) Morrell, D. G.; Kochi, J. K. *J. Am. Chem. Soc.* **1975**, *97*, 7262. (b) McKinney, R. J.; Roe, D. C. *J. Am. Chem. Soc.* **1986**, *108*, 5167. (c) MacGregor, S. A.; Neave, G. W.; Smith, C. *Faraday Discuss.* **2003**, *124*, 111. (d) Lin, B.-L.; Liu, L.; Fu, Y.; Luo, S.-W.; Chen, Q.; Guo, Q.-X. *Organometallics* **2004**, *23*, 2114. (e) Johnson, J. B.; Bercot, E. A.; Rowley, J. M.; Coates, G. W.; Rovis, T. *J. Am. Chem. Soc.* **2007**, *129*, 2718.

(3) (a) Calhorda, M. J.; Brown, J. M.; Cooley, N. A. *Organometallics* **1991**, *10*, 1431. (b) Hartwig, J. F. *Acc. Chem. Res.* **1998**, *31*, 852. (c) Ananikov, V. P.; Musaev, D. G.; Morokuma, K. *J. Am. Chem. Soc.* **2002**, *124*, 2839. (d) Hartwig, J. F. *Inorg. Chem.* **2007**, *46*, 1936. (e) Barder, T. E.; Buchwald, S. L. *J. Am. Chem. Soc.* **2007**, *129*, 12003.

(4) (a) Braterman, P. S.; Cross, R. J.; Young, G. B. *J. Chem. Soc., Dalton Trans.* **1977**, 1892. (b) Abis, L.; Sen, A.; Halpern, J. *J. Am. Chem. Soc.* **1978**, *100*, 2915. (c) Ananikov, V. P.; Musaev, D. G.; Morokuma, K.; Tilset, M.; Van Eldik, R. *Inorg. Chem.* **2006**, *45*, 3613. (e) Gallego, C.; Martinez, M.; Sixte Safont, V. *Organometallics* **2007**, *26*, 527.

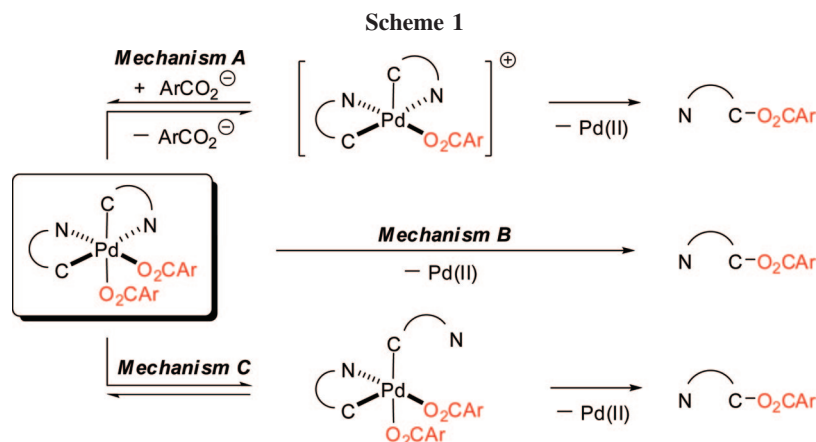
(5) (a) Crumpton, D. M.; Goldberg, K. I. *J. Am. Chem. Soc.* **2000**, *122*, 962. (b) Williams, B. S.; Goldberg, K. I. *J. Am. Chem. Soc.* **2001**, *123*, 2576. (c) Madison, B. L.; Thyme, S. B.; Keene, S.; Williams, B. S. *J. Am. Chem. Soc.* **2007**, *129*, 9538. (d) Pawlikowski, A. V.; Getty, A. D.; Goldberg, K. I. *J. Am. Chem. Soc.* **2007**, *129*, 10382.

(6) (a) Milstein, D.; Stille, J. K. *J. Am. Chem. Soc.* **1979**, *101*, 4981. (b) Duecker-Benfer, C.; van Eldik, R.; Canty, A. J. *Organometallics* **1994**, *13*, 2412. (c) Valk, J.-M.; Boersma, J.; van Koten, G. *Organometallics* **1996**, *15*, 4366. (d) Canty, A. J.; Denney, M. C.; van Koten, G.; Skelton, B. W.; White, A. H. *Organometallics* **2004**, *23*, 5432. (e) Canty, A. J.; Denney, M. C.; Skelton, B. W.; White, A. H. *Organometallics* **2004**, *23*, 1122.

(7) (a) Yoneyama, T.; Crabtree, R. H. *J. Mol. Catal. A* **1996**, *108*, 35. (b) Dick, A. R.; Hull, K. L.; Sanford, M. S. *J. Am. Chem. Soc.* **2004**, *126*, 2300. (c) Desai, L. V.; Hull, K. L.; Sanford, M. S. *J. Am. Chem. Soc.* **2004**, *126*, 9542. (d) Kalyani, D.; Deprez, N. R.; Desai, L. V.; Sanford, M. S. *J. Am. Chem. Soc.* **2005**, *127*, 7330. (e) Hull, K. L.; Lanni, E. L.; Sanford, M. S. *J. Am. Chem. Soc.* **2006**, *128*, 14047. (f) Kalyani, D.; Dick, A. R.; Anani, W. Q.; Sanford, M. S. *Tetrahedron* **2006**, *62*, 11483. (g) Hull, K. L.; Sanford, M. S. *J. Am. Chem. Soc.* **2007**, *129*, 11904.

(8) Related studies: (a) Chen, X.; Li, J.-J.; Hao, X.-S.; Goodhue, C. E.; Yu, J.-Q. *J. Am. Chem. Soc.* **2006**, *128*, 78. (b) Wan, X.; Ma, Z.; Li, B.; Zhang, K.; Cao, S.; Zhang, S.; Shi, Z. *J. Am. Chem. Soc.* **2006**, *128*, 7416. (c) Chiong, H. A.; Pham, Q.-N.; Daugulis, O. *J. Am. Chem. Soc.* **2007**, *129*, 9879. (d) Shi, Z.; Li, B.; Wan, X.; Cheng, J.; Fang, Z.; Cao, B.; Qin, C.; Wang, Y. *Angew. Chem., Int. Ed.* **2007**, *46*, 5554.

(9) Dick, A. R.; Kampf, J. W.; Sanford, M. S. *J. Am. Chem. Soc.* **2005**, *127*, 12790.



the first detailed mechanistic study of C–O reductive elimination from Pd(IV).

Briefly, three distinctly different mechanisms were proposed by Sanford and co-workers to explain the reductive elimination from their Pd(IV) complexes. The first mechanism (mechanism A), which was the most favored by Sanford and co-workers in the beginning, involves a pre-equilibrium dissociation of a benzoate ligand followed by C–O reductive elimination (Scheme 1). In the second mechanism (mechanism B) direct reductive elimination takes place from the six-coordinate starting material. Finally, in the third mechanism (mechanism C) the reductive elimination occurs at a five-coordinate Pd(IV) complex produced by dissociation of a pyridyl arm of one cyclometalated ligand. Through detailed experimental analyses including the solvent effect studies, Eyring and Hammett analyses, and competition reactions,⁹ it was found with great surprise that mechanism A could not be valid for the C–O coupling reaction. Thus it had to be concluded that either mechanism B or C should account for the observed C–O reductive elimination at Pd(IV).

Sanford's experiments indicated that C–O coupling at Pd(IV) proceeds by a dramatically different mechanism than other reductive eliminations from Pd(IV)¹⁰ or Pt(IV) centers.¹¹ This intriguing observation strongly prompted us to carry out the first theoretical study to probe the mechanism of the same C–O bond-forming reductive elimination reactions at Pd(IV).^{12,13} A central question in our study is whether the experimental activation barriers and the solvent and substituent effects can be correctly reproduced by the theory. The consistence between the experiment and theory will provide important insights into the puzzling finding that mechanism B or C prevails over mechanism A in Pd(IV)-mediated C–O coupling. Note that the direct reductive elimination from the octahedral Pd(IV) complex is a very rare process in both Pd(IV) and Pt(IV) chemistry.¹⁴

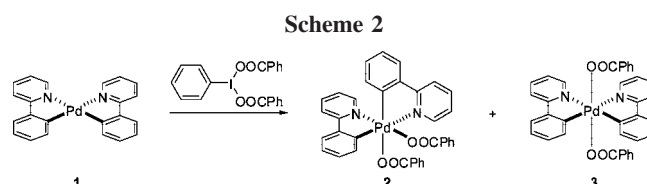
(10) C–C reductive elimination from Pd(IV) typically proceeds by mechanism A, with minimal (<5%) contribution from B or C. See: Byers, P. K.; Cauty, A. J.; Crespo, M.; Puddephatt, R. J.; Scott, J. D. *Organometallics* **1988**, *7*, 1363.

(11) (a) Dick, A. R.; Kampf, J. W.; Sanford, M. S. *Organometallics* **2005**, *24*, 482. (b) Procelewska, J.; Zahl, A.; Liehr, G.; Van Eldik, R.; Smythe, N. A.; Williams, B. S.; Goldberg, K. I. *Inorg. Chem.* **2005**, *44*, 7732.

(12) Reductive elimination of an O–H bond from an η^2 -peroxo-Pd(IV) center was recently discussed in Stahl's computational study on the insertion of O₂ into Pd–H. See: Popp, B. V.; Stahl, S. S. *J. Am. Chem. Soc.* **2007**, *129*, 4410.

(13) For an earlier study on a hypothetical Pd(II)/Pd(IV) cycle of the Heck reaction, see: Sundermann, A.; Uzan, O.; Martin, J. M. L. *Chem.–Eur. J.* **2001**, *7*, 1703.

(14) For rare direct reductive elimination from Pt(IV), see: (a) Luedtke, A. T.; Goldberg, K. I. *Inorg. Chem.* **2007**, *46*, 8496. (b) Crumpton-Bregel, D. M.; Goldberg, K. I. *J. Am. Chem. Soc.* **2003**, *125*, 9442. (c) Edelbach, B. L.; Lachicotte, R. J.; Jones, W. D. *J. Am. Chem. Soc.* **1998**, *120*, 2843.



Furthermore, a second central question in the present study is whether mechanism B or C is more suitable for the observed reductive elimination. A theoretical study concerning this question is of contemporary relevance because mechanisms B and C still remained kinetically indistinguishable from the latest experiments.⁹ The answer to the question may be helpful for the development of new Pd(IV)-catalyzed reactions.

2. Reaction Pathways

2.1. Six-Coordinate Pd(IV) Complexes. The reactants in Sanford's experiments were six-coordinate Pd(IV) complexes carrying two cyclometalated 2-phenylpyridines and two benzoate ligands.⁹ By using the standard B3LYP method (basis set = 6-31G(d) for C, H, O, N and LANL2DZ for Pd)^{15,16} we successfully optimize these Pd(IV) complexes. As for the unsubstituted case, it is found that the two possible isomers of the Pd(IV) complex have significantly different free energies, where the *cis*-isomer **2** is much more stable than the *trans*-isomer **3** by 5.9 kcal/mol in chloroform (Scheme 2). This result is in agreement with Sanford's experiment, because only the *cis*-isomer could be produced from the oxidation reaction.⁹

For the *para*-NO₂ analogue of compound **2** Sanford and co-workers reported the X-ray crystallography data.⁹ Compared to the experimental geometry parameters, our theoretical calculation successfully reproduces the bond lengths within a precision of 0.017 Å and the bond angles within a precision of 1.0° (Figure 1). All the above data indicate that the six-coordinate Pd(IV) complexes can be reliably modeled by the selected theoretical method.

2.2. Mechanism A. According to mechanism A the six-coordinate Pd(IV) complex (**2**) has to discharge a benzoate

(15) de Jong, G. T.; Bickelhaupt, F. M. *J. Chem. Theory Comput.* **2006**, *2*, 322.

(16) Some recent theoretical studies on Pd-catalyzed transformations by using the B3LYP method: (a) Watson, M. P.; Overman, L. E.; Bergman, R. G. *J. Am. Chem. Soc.* **2007**, *129*, 5031. (b) Garcia-Cuadrado, D.; de Mendoza, P.; Braga, A. A.; Maseras, F.; Echavarren, A. M. *J. Am. Chem. Soc.* **2007**, *129*, 6880. (c) Ahlquist, M.; Fabrizi, G.; Cacchi, S.; Norrby, P.-O. *J. Am. Chem. Soc.* **2006**, *128*, 12785. (d) Ariafard, A.; Lin, Z. *J. Am. Chem. Soc.* **2006**, *128*, 13010. (e) Nielsen, R. *J. Am. Chem. Soc.* **2006**, *128*, 9651. (f) Cui, X.; Li, Z.; Tao, C.-Z.; Xu, Y.; Li, J.; Liu, L.; Guo, Q.-X. *Org. Lett.* **2006**, *8*, 2467.

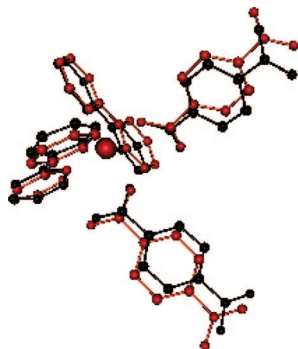


Figure 1. Comparison of the crystal (black) and theoretical (red) structures for the *para*-NO₂ analogue of compound **2**.

ligand in the first step, which gives a five-coordinate Pd(IV) complex as the reaction intermediate (**Int-A1**). The free energy cost of this step is +9.0 kcal/mol, as calculated in chloroform (Figure 2). Note that in **Int-A1** the two cyclometalated pyridine ligands stay at their original locations without much geometry reorganization. Subsequently **Int-A1** rotates its ligand to produce a geometric isomer **Int-A2**, which then undergoes a C–O bond-forming reductive elimination to produce a two-coordinate Pd(II) complex (**Int-A3**) through the transition state **TS-A**. **TS-A** has a free energy of +31.4 kcal/mol in chloroform as compared to the starting material. The product of the above step (i.e., **Int-A3**) carries a single positive charge. It can combine with a free benzoate ligand in the solution to produce a neutral three-coordinate Pd(II) complex (i.e., **Product**, as shown in Figure 1). This finishes the whole reductive elimination reaction, and the overall free energy change of the transformation is –30.1 kcal/mol in chloroform.

Note that in the reductive elimination of mechanism A there are two chemically different C–N ligands. One ligand is on the basal plane, whereas the other occupies both the apical and

one basal site. Our calculation shows that the former C–N ligand has a free energy barrier of +31.4 kcal/mol in the reductive elimination, whereas the latter has a free energy barrier of +41.7 kcal/mol.

2.3. Mechanism B. In mechanism B the six-coordinate Pd(IV) complex (**Reactant**) directly undergoes reductive elimination through a single, six-coordinate transition state (**TS-B**, Figure 3). In **TS-B** the $\angle\text{C–Pd–O}$ angle decreases from 87.2° to 49.1°, while the C–Pd and O–Pd bond lengths increase from 2.04 Å to 2.14 Å and from 2.05 Å to 2.24 Å, respectively. The free energy cost of **TS-B** is calculated to be +26.4 kcal/mol in chloroform. The direct product of mechanism B is a four-coordinate Pd(II) complex (**Int-B**), which will afford the same neutral three-coordinate Pd(II) complex (**Product**) as produced from mechanism A. This finishes the reductive elimination reaction, and the overall free energy change is again –30.1 kcal/mol in chloroform.

2.4. Mechanism C. In mechanism C, the six-coordinate Pd(IV) complex (**Reactant**) releases a pyridyl arm from one of its cyclometalated ligands to form a five-coordinate Pd(IV) intermediate by rotating the C–C bond between the two aromatic rings (**Int-C1**, Figure 4). The free energy cost of this step is +14.1 kcal/mol in chloroform. Subsequently **Int-C1** undergoes reductive elimination through a five-coordinate transition state (**TS-C**). In **TS-C** the $\angle\text{C–Pd–O}$ angle is 54.3°, while the C–Pd and O–Pd bond lengths are 2.24 and 2.11 Å, respectively. The free energy cost of **TS-C** is calculated to be +44.3 kcal/mol relative to **Reactant** in chloroform. The direct product of mechanism C is a four-coordinate Pd(II) complex (**Int-C2**), which again produces the same neutral three-coordinate Pd(II) complex (**Product**) as produced from mechanisms A and B.

2.5. The Favored Mechanism. In all of the three possible mechanisms examined in the above sections, it is found that the rate-limiting step is the reductive elimination to form the

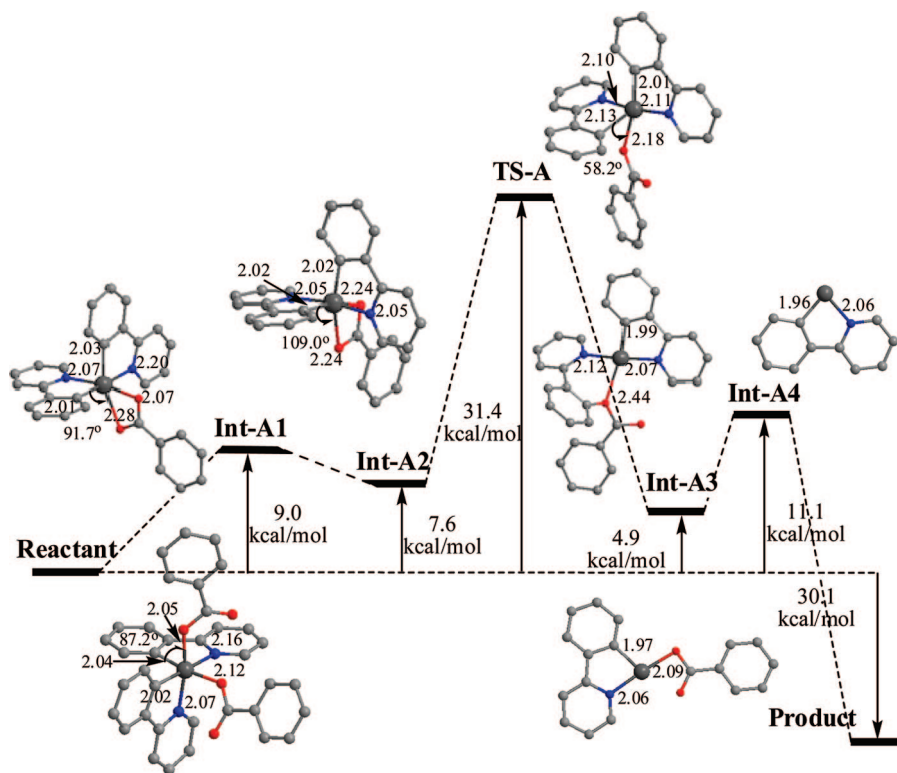


Figure 2. Free energy profile for mechanism A (all the free energies are relative values as compared to **Reactant**).

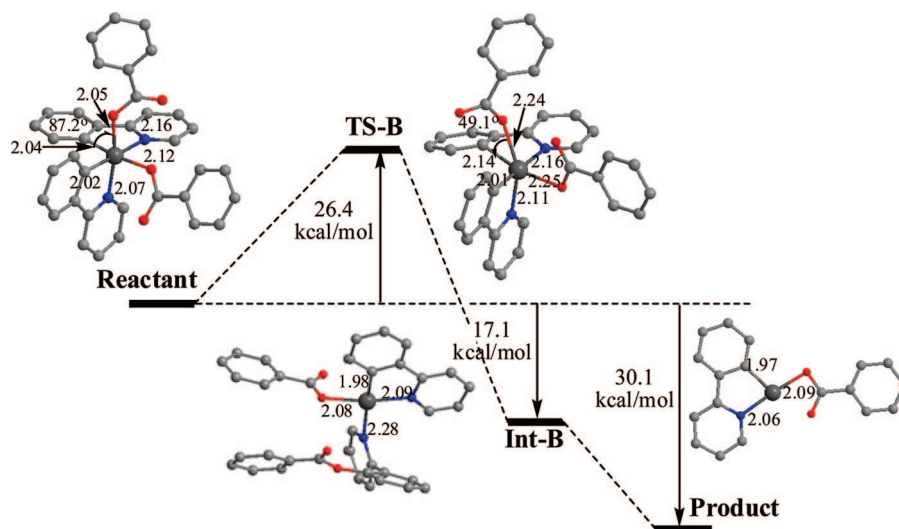


Figure 3. Free energy profile for mechanism B (all the free energies are relative values as compared to **Reactant**).

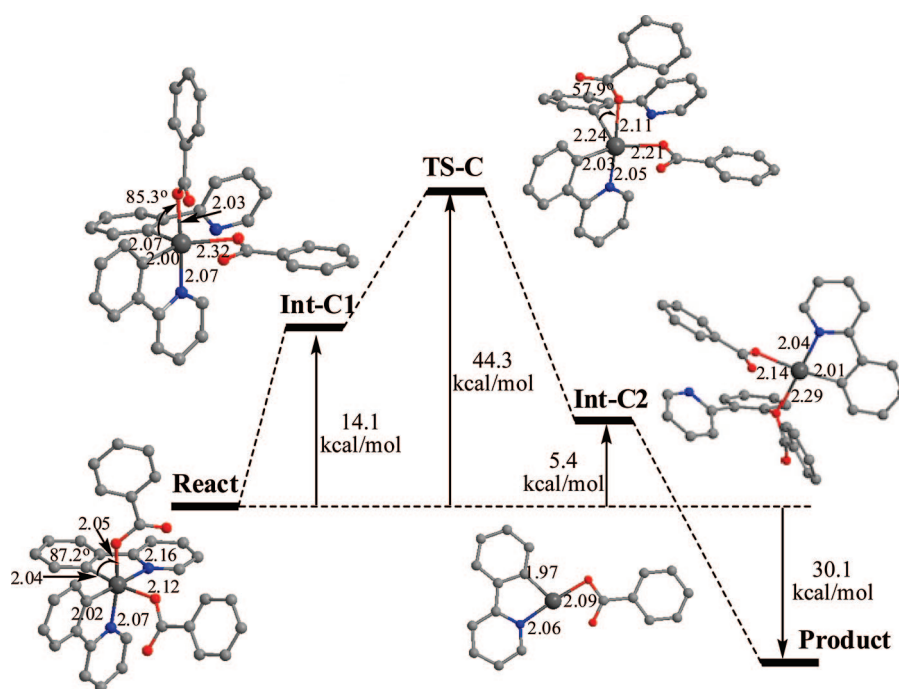


Figure 4. Free energy profile for mechanism C (all the free energies are relative values as compared to **Reactant**).

Table 1. Free Energies of the Aforementioned Species in Chloroform (kcal/mol) and the Corresponding Rate Constants (s^{-1})

species	ΔG	ΔG_{solv}	$\Delta G + \Delta G_{\text{solv}}$	k_{calc}	k_{exp}
Reactant	0.0	0.0	0.0		6.4×10^{-4}
Int-A1	81.0	-72.0	9.0		
Int-A2	80.5	-72.8	7.6		
TS-A	104.3	-72.9	31.4	1.8×10^{-8}	
Int-A3	75.1	-70.3	4.9		
Int-A4	117.8	-106.7	11.1		
TS-B	25.3	1.1	26.4	3.1×10^{-5}	
Int-B	-18.7	1.6	-17.1		
Int-C1	13.7	0.4	14.1		
TS-C	42.0	2.3	44.3	5.7×10^{-17}	
Int-C2	1.7	3.7	5.4		
Product	-23.8	-6.4	-30.1		

new C–O bond. The corresponding free energy barriers in chloroform are calculated to be +31.4, +26.4, and +44.3 kcal/mol for mechanisms A, B, and C (Table 1). According to transition-state theory with the transmission coefficient equated

to unity, the above free energies can be translated to the first-order rate constants of 1.8×10^{-8} , 3.1×10^{-5} , and $5.7 \times 10^{-17} s^{-1}$ at 60 °C, respectively. Note that the experimental rate constant was reported by Sanford et al. to be ca. $6.4 \times 10^{-4} s^{-1}$ at 60 °C in chloroform.⁹ Thus our theoretical calculation appears to support mechanism B, where the relatively small difference between the calculated and experimental rate constants (i.e., 3.1×10^{-5} vs $6.4 \times 10^{-4} s^{-1}$) can be attributed to the inevitable error bar (ca. 1–2 kcal/mol) of the current quantum chemistry methods in dealing with complexed reaction systems.

Note that, from the electronic effect consideration, reductive elimination is more likely to occur at a positively charged, five-coordinate Pd(IV) center. However, our above calculations show that mechanism B (+26.4 kcal/mol) has a lower free energy barrier than mechanism A (+31.4 kcal/mol). This hypothesis was previously indicated by Sanford's experiments (including the solvent effect studies, Eyring and Hammett analyses, and

Table 2. Free Energies in Different Solvents (kcal/mol) and the Corresponding Rate Constants (s⁻¹)

solvent	species	ΔG	ΔG_{solv}	$\Delta G + \Delta G_{\text{solv}}$	k_{calc}
CHCl ₃	Reactant	0.0	0.0	0.0	3.1×10^{-5}
	TS-B	25.3	1.1	26.4	
	Product	-23.8	-6.4	-30.1	
DMSO	Reactant	0.0	0.0	0.0	2.4×10^{-5}
	TS-B	25.3	1.3	26.6	
	Product	-23.8	-8.0	-31.8	

Table 3. Free Energy Barriers for the Reductive Elimination of Pd(IV) Complexes of Different Benzoates in CHCl₃ (kcal/mol) and the Corresponding Rate Constants (s⁻¹)

Mechanism B
- Pd(II)

benzoate	σ_p	ΔG^\ddagger	k_{exp}	log ($k_{\text{R}}/k_{\text{H}}$) _{exp}	k_{calc}	log ($k_{\text{R}}/k_{\text{H}}$)
H-C ₆ H ₄ -COO ⁻	0.00	26.4	6.4×10^{-4}	0.00	3.1×10^{-5}	0.00
4-Me-O-C ₆ H ₄ -COO ⁻	-0.27	25.1	1.4×10^{-3}	0.34	2.4×10^{-4}	0.88
4-Me-C ₆ H ₄ -COO ⁻	-0.17	25.6	8.5×10^{-4}	0.12	1.1×10^{-4}	0.56
4-F-C ₆ H ₄ -COO ⁻	0.06	25.8	3.6×10^{-4}	-0.25	8.0×10^{-5}	0.41
4-Cl-C ₆ H ₄ -COO ⁻	0.23	26.2	2.7×10^{-4}	-0.37	4.6×10^{-5}	0.17
4-Br-C ₆ H ₄ -COO ⁻	0.23	26.8	3.1×10^{-4}	-0.31	2.0×10^{-5}	-0.20
4-Ac-C ₆ H ₄ -COO ⁻	0.45	26.6	2.0×10^{-4}	-0.51	2.6×10^{-5}	-0.08

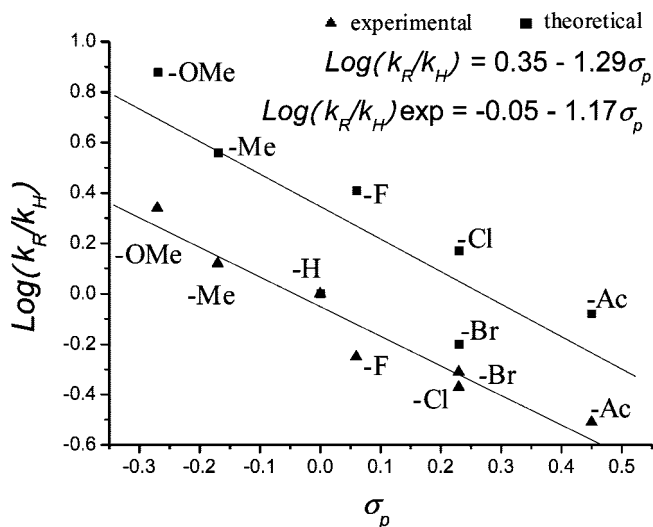
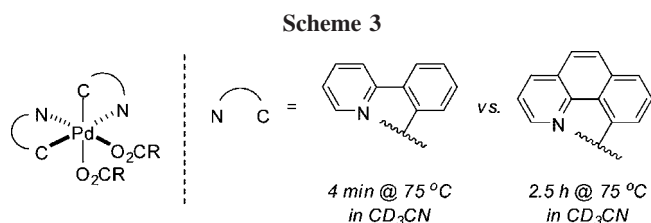
competition reactions).⁹ A major driving force may exist to favor the reductive elimination from a six-coordinate Pd(IV). Since electronic effects is not the reason, we can only argue that the steric crowding of the six-coordinate Pd(IV) may constitute an important driving force for the reductive elimination to produce a less crowded, four-coordinate Pd(II) complex.

3. Discussion

3.1. Solvent Effect. In Sanford's experiments it was found that the effect of solvent polarity on the rate of C–O reductive elimination was very small.⁹ This observation was used as important evidence to exclude mechanism A because the rates of ionic reductive elimination from both Pt(IV) and Pd(IV) were known to exhibit strong dependence on solvent polarity.^{5,10} Here our calculations show that the free energy barriers of reductive elimination in CHCl₃ (low polarity, $\epsilon = 4.8$) and DMSO (high polarity, $\epsilon = 47$) are 26.4 and 26.6 kcal/mol, respectively (Table 2). These values are translated to the rate constants 3.1×10^{-5} and 2.4×10^{-5} s⁻¹, whose relative ratio (2.5:2.0) is close to Sanford's experimental ratio (2.3:2.0).⁹ Thus the calculated solvent effect is consistent with the experimental results.

3.2. Substituent Effect. Because benzoates are used as ligands in the Pd(IV) complexes, the effect of the remote aromatic substituents on the rate of C–O reductive elimination can provide further information about the validity of the proposed mechanism. In Sanford's experiment it was found that electron donor substituents led to moderate rate accelerations with a Hammett ρ value of -1.36 .⁹ This observation indicated that the benzoate acted as a nucleophilic partner in the C–O reductive elimination. On the other hand, C–O reductive elimination from Pt(IV) (which proceeds via mechanism A) shows a Hammett ρ value of $+1.44$, indicative of stabilization of the dissociated benzoate moiety by electron-withdrawing groups.⁵

Here we examine whether our theoretical model can correctly reproduce the experimental substituent effects. To this end we have calculated the free energy barriers for the reductive elimination of the Pd(IV) complexes of different benzoates in CHCl₃ (Table 3). From these free energy barriers we next

**Figure 5.** Hammett plot for Pd(IV) benzoates.

estimate the corresponding rate constants (k_{calc}) by using the transition-state theory with the transmission coefficient equated to unity. The relative value ($\log(k_{\text{R}}/k_{\text{H}})$) between the rate constant of unsubstituted and substituted benzoates is then readily obtained. These relative values are subsequently plotted against the Hammett substituent constants σ_p ¹⁷ (Figure 5), from which it is determined that the theoretical Hammett ρ value for the reductive elimination from Pd(IV) is -1.29 . This predicted value is in good agreement with the experimental Hammett ρ value (-1.17)⁹ and, therefore, supports Sanford's proposed mechanism.

3.3. Effect of Different C–N Ligands. Although our above calculations favor mechanism B over mechanism C, it should be pointed out that these two mechanisms remain kinetically indistinguishable from the available experiments. Nonetheless, Sanford and co-workers measured the rate of reductive elimination from a Pd(IV) complex of bisphenylpyridine to that from a bisbenzo[*h*]quinoline complex (Scheme 3).⁹ It was argued that, in the case of mechanism B, comparable rates of reductive elimination should be expected due to the similar steric and electronic parameters of the ligands. Therefore, the dramatic difference between the two observed rates led Sanford and co-workers to propose that mechanism B should be ruled out.

Here we want to show that Sanford's experimental observations for the above two different C–N ligands are not conflicting with mechanism B. To this end we use the same theoretical methods as used for the bisphenylpyridine complex to model the reductive elimination from the bisbenzo[*h*]quinoline complex (Figure 6). It is found that the free energy barriers for the reductive elimination from the bisbenzo[*h*]quinoline and bisphenylpyridine complexes are $+29.0$ and $+26.4$ kcal/mol in acetonitrile, respectively. These two free energy barriers are translated to first-order rate constants of 4.4×10^{-6} and $1.9 \times$

(17) (a) Hansch, C.; Leo, A.; Tafts, R. M. *Chem. Rev.* **1991**, *91*, 165. (b) Liu, L.; Fu, Y.; Liu, R.; Li, R.-Q.; Guo, Q.-X. *J. Chem. Inf. Comput. Sci.* **2004**, *44*, 652.

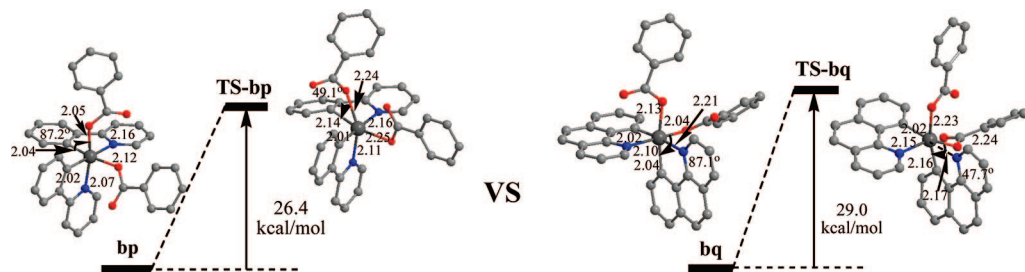


Figure 6. Reductive elimination from a Pd(IV) complex of bisphenylpyridine as compared to that from the bisbenzo[*h*]quinoline complex.

10^{-4} s^{-1} at $75 \text{ }^\circ\text{C}$ (or half-lives of 43.8 and 1.0 h). Note that the theoretical half-lives are about one magnitude higher than the experimental ones, where the reactions were observed to complete after ca. 2.5 h and 4 min.⁹ This is explained in Section 2.5 as the result of the inevitable error bar (ca. 1–2 kcal/mol) of the present quantum chemistry methods in dealing with complexed reaction systems. Nevertheless, the ratio between the two theoretical half-lives (i.e., 43.8) is consistent with the experimental ratio (i.e., 2.5 h:4 min = 37.5), indicating that the current theory is sufficient to predict the relative reactivities.

The above theoretical result shows that mechanism B is compatible with Sanford's experiment. From the theoretical study we have also identified the cause of the dramatically different reductive elimination rates of the two complexes. As shown in Figure 6, in the Pd(IV)–bisphenylpyridine complex the phenylpyridine ring is fully planar. However, in the transition state (**TS-bp**) the two aromatic rings are distorted from each other with a $\angle\text{C-C-C-N}$ dihedral angle of 160.1° . This distortion appears to facilitate the shortening of the $\text{C}\cdots\text{O}$ distance. By comparison, in the Pd(IV)–bisbenzo[*h*]quinoline complex the benzo[*h*]quinoline ring is also fully planar, but in the transition state (**TS-bq**) the benzo[*h*]quinoline displays much less distortion, with a $\angle\text{C-C-C-N}$ dihedral angle of 171.3° . Less tolerance of the distortion means smaller room for the geometry reorganization that is needed to minimize the free energy. As a result, the added rigidity of the fused ring system decreases the rate of the reductive elimination from Pd(IV).¹⁸

4. Summary

Carbon–oxygen bond-forming reductive elimination from transient Pd(IV) aryl/acetate complexes was recently implicated as the product release step in Pd(II)-catalyzed arene oxygenation reactions. The mechanistic details of C–O bond formation from these Pd(IV) intermediates remain elusive and, therefore, are subjected to a theoretical investigation in the present study. Three proposed mechanisms are examined including (A) pre-equilibrium dissociation of a benzoate ligand followed by reductive elimination from the resulting five-coordinate Pd(IV); (B) direct reductive elimination from the six-coordinate Pd(IV); and (C) dissociation of a pyridyl arm of one cyclometalated ligand followed by internal coupling. Through density functional theory calculations it is concluded that mechanism B is favored over the other two mechanisms. This conclusion is supported by the success of the theoretical model to reproduce the experimental activation barriers and to reproduce the solvent and substituent effects on the reductive elimination rate. Furthermore, our calculations explain why the rate of reductive

elimination from the bisphenylpyridine complex is significantly faster than that from bisbenzo[*h*]quinoline. Accordingly mechanism C is not supported by the theory.

5. Computational Methodology

All the calculations were performed with the Gaussian 03 programs¹⁹ using our HP Superdome Sever ($32 \times 1.5 \text{ GHz}$ Itanium 2 Madison CPU). Initial geometry optimization was carried out using the B3LYP²⁰ density functional and an effective core potential (LANL2DZ+p) for Pd.²¹ The basis set for the other elements including H, C, N, and O is 6-31G(d). Each optimized structure was confirmed by the frequency calculation at the same level to be the real minimum without any imaginary vibration frequency. For compounds that have multiple conformations, efforts were made to find the lowest energy conformation by comparing the structures optimized from different starting geometries.

Harmonic vibrational frequencies were calculated using the B3LYP/LANL2DZ+p method from the optimized geometries. Zero-point vibrational energy (ZPE) corrections were obtained using unscaled frequencies. Single-point electronic energies were then calculated at the PBEPBE/BS2 level (BS2: the basis set for Pd is LANL2DZ+p, and the basis set for the other elements including H, C, N, O is 6-311G(d,p)). Gas-phase free energy change was corrected with ZPE, thermal corrections, and the entropy terms. Note that all the calculated gas-phase free energies corresponded to the reference state of 1 atm, 333 or 348 K.

In order to examine the solvation effect, we utilized the IEF-PCM solvation model at the B3LYP/LANL2DZ+p level (version = Matrix Inversion, cavity = GePol, TSARE = 0.2, radii = UA0, alpha = 1.0).²³ The gas-phase geometry was used for all of the solution-phase calculations, because it has been demonstrated in many previous studies that the change of geometry by the solvation effect is usually not significant.²⁰ It is worth noting that all the

(19) Frisch, M. J.; Trucks, G. W.; Schlegel, H. B.; Scuseria, G. E.; Robb, M. A.; Cheeseman, J. R.; Montgomery, J. A., Jr.; Vreven, T.; Kudin, K. N.; Burant, J. C.; Millam, J. M.; Iyengar, S. S.; Tomasi, J.; Barone, V.; Mennucci, B.; Cossi, M.; Scalmani, G.; Rega, N.; Petersson, G. A.; Nakatsuji, H.; Hada, M.; Ehara, M.; Toyota, K.; Fukuda, R.; Hasegawa, J.; Ishida, M.; Nakajima, T.; Honda, Y.; Kitao, O.; Nakai, H.; Klene, M.; Li, X.; Knox, J. E.; Hratchian, H. P.; Cross, J. B.; Adamo, C.; Jaramillo, J.; Gomperts, R.; Stratmann, R. E.; Yazyev, O.; Austin, A. J.; Cammi, R.; Pomelli, C.; Ochterski, J. W.; Ayala, P. Y.; Morokuma, K.; Voth, G. A.; Salvador, P.; Dannenberg, J. J.; Zakrzewski, V. G.; Dapprich, S.; Daniels, A. D.; Strain, M. C.; Farkas, O.; Malick, D. K.; Rabuck, A. D.; Raghavachari, K.; Foresman, J. B.; Ortiz, J. V.; Cui, Q.; Baboul, A. G.; Clifford, S.; Cioslowski, J.; Stefanov, B. B.; Liu, G.; Liashenko, A.; Piskorz, P.; Komaromi, I.; Martin, R. L.; Fox, D. J.; Keith, T.; Al-Laham, M. A.; Peng, C. Y.; Nanayakkara, A.; Challacombe, M.; Gill, P. M. W.; Johnson, B.; Chen, W.; Wong, M. W.; Gonzalez, C.; Pople, J. A. *Gaussian 03*, revision B.04; Gaussian, Inc.: Pittsburgh, PA, 2003.

(20) (a) Becke, A. D. *Phys. Rev. A* **1988**, *38*, 3098. (b) Becke, A. D. *J. Chem. Phys.* **1993**, *98*, 1372. (c) Becke, A. D. *J. Chem. Phys.* **1993**, *98*, 5648.

(21) Hay, P. J.; Wadt, W. R. *J. Chem. Phys.* **1985**, *82*, 299.

(22) Paier, J.; Marsman, M.; Kresse, G. *J. Chem. Phys.* **2007**, *127*, 24103.

(18) For related discussion on the effect of geometry reorganization on Pd catalysis, see: (a) Legault, C. Y.; Garcia, Y.; Merlic, C. A.; Houk, K. N. *J. Am. Chem. Soc.* **2007**, *129*, 12664.

calculated solution-phase free energies correspond to the reference state of 1 mol/L, 333 or 348 K.

(23) (a) Cramer, C. J.; Truhlar, D. G. *Chem. Rev.* **1999**, *99*, 2161. (b) Tomasi, J.; Mennucci, B.; Cammi, R. *Chem. Rev.* **2005**, *105*, 2999. (c) Fu, Y.; Liu, L.; Yu, H.-Z.; Wang, Y.-M.; Guo, Q.-X. *J. Am. Chem. Soc.* **2005**, *127*, 7227. (d) Qi, X.-J.; Liu, L.; Fu, Y.; Guo, Q.-X. *Organometallics* **2006**, *25*, 5879. (e) Qi, X.-J.; Fu, Y.; Liu, L.; Guo, Q.-X. *Organometallics* **2007**, *26*, 4197.

Acknowledgment. We thank NSFC (No. 20602034) for the financial support. We also thank Mr. Xiao-Cong Wang for some preliminary calculations.

Supporting Information Available: Detailed optimized geometries and free energies. This material is available free of charge via the Internet at <http://pubs.acs.org>.

OM800067U